Ultrafast Self-Induced X-Ray Transparency and Loss of Magnetic Diffraction

Z. Chen,[1] D. J. Higley,[2] M. Beye,[3] M. Hantschmann,[4] V. Mehta,[5] O. Hellwig,[6, 7] A. Mitra,[8, 9]
S. Bonetti,[10] M. Bucher,[8] S. Carron,[8] T. Chase,[11] E. Jal,[8] R. Kukreja,[12] T. Liu,[1] A. H.
Reid,[8] G. L. Dakovski,[8] A. Föhlisch,[4] W. F. Schlotter,[8] H. A. Dürr,[8, 13] and J. Stöhr[14, *]

[1]*Dept. of Physics, Stanford University, Stanford, CA 94305, USA*
[2]*Dept. of Applied Physics, Stanford University, Stanford, CA 94305, USA*
[3]*Dept. of Photon Science, DESY, Notkestraße 85, D-22607 Hamburg, Germany*
[4]*Dept. of Materials and Energy Science, Helmholtz Zentrum Berlin, D-14109 Berlin, Germany*
[5]*San Jose Research Center, HGST a Western Digital company, San Jose, CA 95135, USA*
[6]*Institute of Physics, Technische Universität Chemnitz, D-09107 Chemnitz, Germany*
[7]*Institute of Ion Beam Physics and Materials Research,*
Helmholtz-Zentrum Dresden-Rossendorf, 01328 Dresden, Germany
[8]*SLAC National Accelerator Laboratory, 2575 Sand Hill Road, Menlo Park, CA 94025, USA*
[9]*Department of Physics, University of Warwick, Coventry; United Kingdom*
[10]*Dept. of Physics, Stockholm University, S-10691 Stockholm, Sweden*
[11]*Dept. of Applied Physics, Stanford University, Stanford, CA, 94305 USA*
[12]*Dept. of Mat. Sci. and Eng., University of California Davis, Davis, CA 95616, USA*
[13]*Department of Physics and Astronomy, Uppsala University, BOX 516, 75120 Uppsala, Sweden*
[14]*SLAC National Accelerator Laboratory and Dept. of Photon Science, Stanford, CA 94035, USA*
(Dated: September 17, 2018)

Using ultrafast $\simeq 2.5$ fs and $\simeq 25$ fs self amplified spontaneous emission pulses of increasing intensity and a novel experimental scheme, we report the concurrent increase of stimulated emission in the forward direction and loss of out-of-beam diffraction contrast for a Co/Pd multilayer sample. The experimental results are quantitatively accounted for by a statistical description of the pulses in conjunction with the optical Bloch equations. The dependence of the stimulated sample response on the incident intensity, coherence time and energy jitter of the employed pulses reveals the importance of increased control of x-ray free electron laser radiation.

PACS numbers 75.70.-i, 75.50-Cc, 78.70.-Dm

With the advent of x-ray free electron lasers (XFELs), studies of the fundamental physics driving non-linear electronic responses of matter have become possible and research in this area is undergoing rapid progress. An example is the demonstration of the stimulated amplification of spontaneous emission [1–3] and stimulated x-ray Raman scattering [4].

Particular important x-ray processes involve *resonant* excitations of electrons from a core shell to empty valence states, which maximize cross-sections and provide atomic, chemical [5] and magnetic [6] specificity. In conventional experiments, resonant excitations are followed by the *spontaneous* emission of Auger electrons or characteristic x-rays, with Auger decay resulting in irreversible conversion of photons into electrons. The fraction of radiative decays, the x-ray fluorescence yield, is only about 1% for the K-shell of the chemically important low-Z elements C, N and O and the L-shell of the important $3d$ transition metals such as Fe, Co, Ni and Cu [7]. XFEL radiation can overcome this problem through impulsive stimulation via the incident beam itself, whereby Auger decays are replaced by the incident-field-driven stimulated emission of photons.

The experiment reported here utilizes the innovative experimental arrangement shown in Fig. 1 to directly reveal the hallmark of stimulated emission, namely the enhancement of the intensity in the forward direction. It also allows us to observe, pulse-by-pulse, the interplay between the *increase* of the transmitted in-beam intensity and the *decrease* of the out-of-beam diffracted intensity as a result of power conservation [8, 9]. A previous experiment only revealed the indirect effect of reduced diffraction, but the key signature of stimulated enhancement was hidden due to a beam stop blocking transmission of the main beam [10].

We utilize self-amplified spontaneous emission (SASE) pulses of <25 fs over an intensity range covering three orders of magnitude. Our experimental results are quantitatively reproduced by simulations that account for the statistical variations of the SASE pulses. They demonstrate the importance of controlling stimulated emission through intensity stability, photon energy tuning, and coherence times that exceed the core hole lifetime by about a factor of 10. This is shown by comparing the threshold of stimulated emission for unprocessed SASE pulses with a coherence time $\simeq 1$ fs to monochromatized pulses with coherence times around $\simeq 10$ fs [10].

We used magnetic Co/Pd multilayer samples deposited via sputtering on SiN windows with a metal layer sequence Ta(1.5)/Pd(3)/[Co(1)Pd(0.7)]x25/Pd(2), where thickness values are in nm. As part of the fabrication process, the samples were placed in an oscillatory in-plane

---

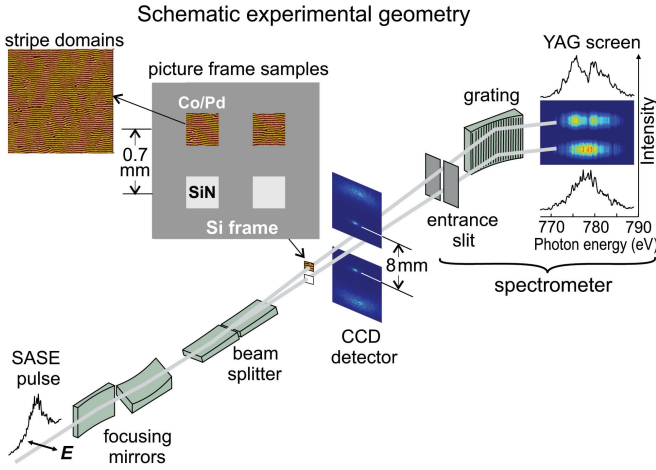*Electronic address: Email:stohr@stanford.edu

FIG. 1: (color online) Experimental geometry for simultaneous pulse-by-pulse measurements of the transmitted and diffracted response of a Co/Pd thin film. Incident SASE pulses of ~ 2.5 fs or ~ 25 fs length are focused onto the sample plane and split by the sharp edge of a mirror, with one half propagating through a Co/Pd/SiN sample in a picture frame and the other through a pure SiN reference film for normalization purposes. The horizontal magnetic stripe domains in Co/Pd produce strong first and third order Bragg diffraction peaks on a pnCCD detector [11]. The spatially separated undiffracted beams are allowed to propagate into a downstream spectrometer. A grating disperses the two offset beams onto a yttrium aluminum garnet (YAG) fluorescence screen, yielding separate single-shot sample and reference spectra around the Co L_3 resonance. The shown spectra and diffraction images are real data averaged over several pulses.

magnetic field with field strength slowly attenuated every cycle. Such a process created well-defined magnetic stripes of ~ 150nm width at remanence, as shown in Fig. 1, which enhance the diffracted signal relative to the random domains used previously [10]. Samples containing a total of 25 nm Co had $\simeq 30\%$ transmission at the Co L_3 resonance.

Linearly polarized SASE pulses of either ~ 2.5 fs or ~ 25 fs temporal length and ~ 5 eV total width were generated at the Linac Coherent Light Source (LCLS) and steered into the AMO endstation [12]. The central energy of the x-ray pulses was set to the nominal Co L_3 resonance of 778 eV and rastered through modulation of the electron beam energy to cover a range of ~ 20 eV. A calibrated gas detector provided an absolute measure of the integrated incident intensity I_{ref} for each pulse. A sharp-edged mirror split the SASE pulse into two statistically identical halves [13] which then are transmitted through two spatially offset 300μm-wide picture frames: one containing a Co/Pd/SiN sample and one containing a pure SiN membrane for reference. A pair of upstream Kirkpatrick-Baez mirrors focused the beam to $\sim 15 \mu$m diameter spots in the sample plane, as verified by a pinhole scan.

Two movable halves of a pnCCD imaging detector intercepted the first and third-order diffraction pattern of

the magnetic stripe domains, with a 8 mm separation of the first order diffraction spots. We primarily analyze the integrated first order diffracted intensity, denoted I_{d}, but the first and third order intensities closely tracked each other.

The centrally transmitted beam from both the Co/Pd sample, $I_{\text{t}}(\hbar\omega)$, and the reference beam through the SiN membrane, $I_0(\hbar\omega)$, passed through a gap between the two halves of the pnCCD detectors. Their energy-resolved spectra were recorded by a grating spectrometer which dispersed the intensity with a resolving power of ~ 1000 onto an optically fluorescent YAG crystal imaged by a camera.

All intensities were first normalized to the *absolute* integrated incident intensity I_{ref}. A second *relative* pulse-by-pulse normalization was then accomplished by use of the energy resolved reference spectrum $I_0(\hbar\omega)$ of the centrally transmitted reference beam, yielding the central spectroscopy signal $S_{\text{t}}(\hbar\omega) = I_{\text{t}}/I_0$ and the diffracted contrast signal $S_{\text{d}} = I_{\text{d}}/I_0$. The extraction of the spectroscopy signal $S(\hbar\omega) = I_{\text{t}}(\hbar\omega)/I_0(\hbar\omega)$ had to be refined because the reference spectrum $I_0(\hbar\omega)$ dropped to zero near the end of the scan range $\mathcal{E}_0 \pm 10$ eV as shown on the top right of Fig. 1.

To eliminate singularities we therefore show in Fig. 2 the signal $S(\hbar\omega) = C[S'(\hbar\omega) - 1] + 1$ where $S'(\hbar\omega) = (I'_{\text{t}} + C)/(I'_0 + C)$ and $C = 10 \gg I'_{\text{t}}, I'_0$. This normalization scheme emphasizes the behavior of the transmitted signal near resonance. While an incoming intensity of 42 mJ/cm^2/fs produces a prominent L_3 absorption feature, as expected in the linear regime, an increase in intensity reduces the resonance and at 1600 mJ/cm^2/fs no absorption feature can be discerned.

The change in the centrally transmitted intensity revealed by Fig. 2 is replotted as a function of incident intensity as solid blue circles connected by a blue line in Fig. 3. Due to the poor statistics of the spectrometer signal the shown data points represent an average over several shots. In the lower panel of the figure we also show on the same intensity scale the change of the magnetic diffraction contrast as solid red circles. In this case all points represent single shots.

The changes of the in-beam transmitted and out-of-beam diffracted signals shown in Fig. 3 may potentially contain contributions from different microscopic mechanisms. Firstly, the energy deposited in the core excitations can be quickly released into the electronic system on the femtosecond timescale via Auger decays and ensuing electron-electron scattering [14]. The resultant reshuffling of valence electrons across the Fermi edge could lead to a decrease in absorption at the Co resonance and hence an increase of transmission. Secondly, ultrafast demagnetization could completely reduce the magnetic diffraction contrast on a longer timescale of > 200 fs [15], but small changes [16] may be present on the 2.5–25 fs timescale of our pulses. Thirdly, impulsive (by the beam itself) stimulated elastic forward scattering has previously been shown to reduce absorption (increase transmission) at the
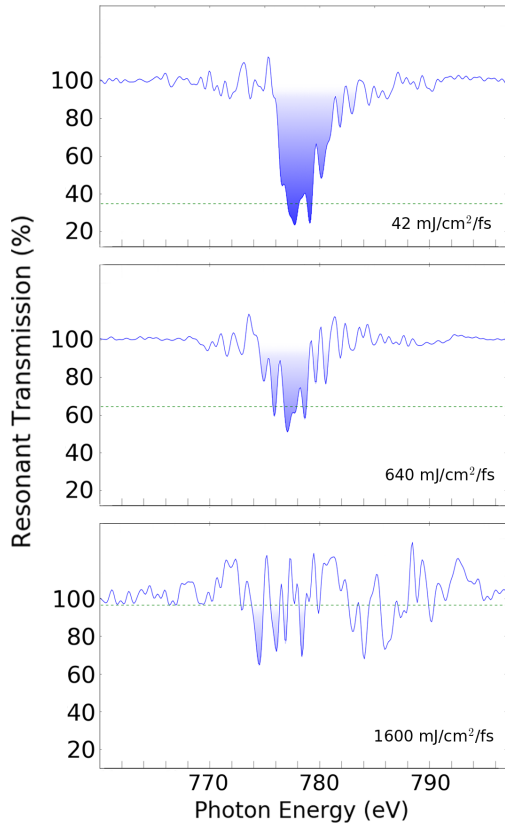
FIG. 2: (color online) Normalized transmission signal $S = C(S' - 1) + 1$ defined in the text for three different incident intensities around the Co L_3 resonance for a Co/Pd multilayer sample. Each spectrum represents an averaged spectrum across multiple shots in a certain fluence range. With increasing intensity the absorption peak (clearly visible at lower intensities) is suppressed and has vanished at the highest intensity of $1600\,\mathrm{mJ/cm^2/fs}$, revealing x-ray transparency.

expense of out of beam diffraction [8, 10].

While contributions of valence electron reshuffling and ultrafast demagnetization cannot be excluded, we show here that our observations are remarkably consistent with a theory of stimulated forward scattering. This model extends well-established quantum optical concepts to the x-ray regime by modeling the electronic structure of the sample as a two-level system where resonant transitions occur between the $2p_{3/2}$ core and empty $3d$ valence states.

In the stimulated scattering model [8, 10], the interplay between resonant absorption and stimulated elastic scattering is well described by the optical Bloch equations for a two-level system. Each atom forms a two-level system with core and valence levels representing the lower and upper energy states, respectively. Before arrival of the x-ray pulse, only the lower state is populated, expressed by a population $\rho_{11} = 1$, while the upper state has a population $\rho_{22} = 0$, where $\rho_{11} + \rho_{22} = 1$. With increasing incident intensity the solutions of the Bloch equations determine
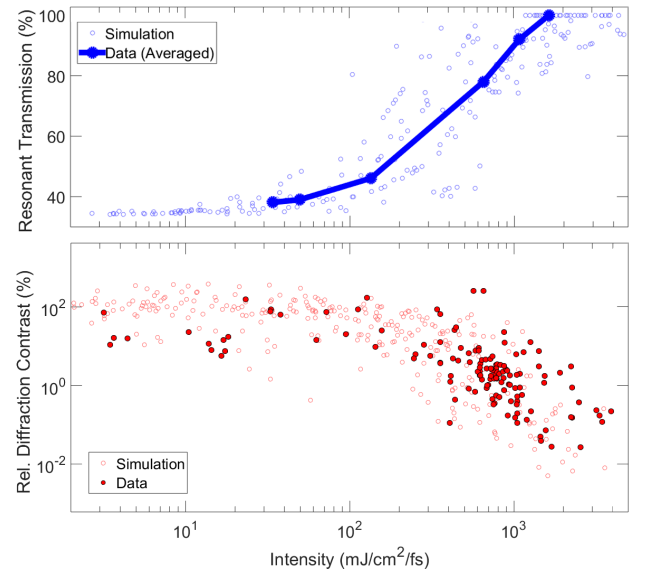

FIG. 3: (color online) Top: Experimentally observed change in the transmitted intensity as a function of incident intensity (solid blue circles and line). Each data point is an average over multiple shots. The open blue circles correspond to the simulated shot-by-shot response using the stimulated forward scattering model discussed in the text. Bottom: Observed shot-by-shot out-of-beam diffracted intensity due to magnetic domains (solid red circles) plotted on a log scale to emphasize the large statistical noise due to the used SASE pulses. Simulated data are shown as open red circles. The shown experimental and simulated data consist of an equal number of single-shot pulses of 2.5 fs and 25 fs duration.

the changes of the populations toward the equilibrium limit $\rho_{11} = \rho_{22} = 0.5$.

The population equilibrium, where there is a complete balance between up and down transitions, is reliably reached if the incident energy is tuned to the exact resonance value and the incident fields have a coherence time τ_{coh} longer than the core hole life time $t_\Gamma = \hbar/\Gamma$, where Γ is the total spontaneous (Auger plus radiative) energy decay width of the core hole ($\Gamma = 0.43\,\mathrm{eV}$ and $t_\Gamma = 1.5\,\mathrm{fs}$ for Co L_3). This was accomplished in a previous study [10] by use of a monochromator which by energy filtering of the incident SASE pulses fixed the incident photon energy to the resonance value $\mathcal{E}_0$ and the resulting small bandwidth $\Delta\mathcal{E}_0 \simeq 0.2\,\mathrm{eV}$ yielded a sufficiently long coherence time of about 10 fs. For the case of a thin film one also needs to consider that the total atomic system of areal number density N_a/A responds coherently, lowering the stimulated onset by a value of $\mathcal{G}_{\mathrm{coh}} = N_a\lambda^2/(4\pi A)$, where λ is the wavelength. For the Co L_3 resonance in Co metal we have $\mathcal{G}_{\mathrm{coh}} \simeq 360$ [8].

In the present study, no monochromator was used so that the pulses had an intrinsic coherence time $\tau_{\mathrm{coh}} \sim 1\,\mathrm{fs}$ associated with the spikes in the incident SASE pulses. In addition, as each SASE pulse has $\sim 5\,\mathrm{eV}$ width, most photons within each pulse are detuned from the resonance

energy. SASE pulses of specified pulse length and central intensity were simulated as described in [17]. The simulations yield a parameter set $I_0, \tau_{\rm coh}, \Delta\mathcal{E}$ for each *spike* within the total SASE pulse, where $\Delta\mathcal{E} = \hbar\omega - \mathcal{E}_0$ is the detuning energy from resonance. We assumed *independent* SASE spikes and solved the optical Bloch equations for each coherent spike, with the total pulse response being the sum of the individual spike responses. Inhomogeneous broadening effects were taken into account as prescribed by [18, 19]. Examples of simulated SASE pulses for various beam parameters are shown in the inset of Figure 4 below. The simulations gave a histogram of coherence times peaked in the $\tau_{\rm coh} \simeq 0.5-1$ fs range for both 2.5 fs and 25 fs pulses in good accord with experimental results [20]. The stimulated response was therefore similar for both pulse lengths with the larger number of spikes in the 25 fs pulses simply yielding a better defined statistical average (see below).

Solution of the optical Bloch equations yielded the pulse averaged excited state population $\rho_{22}(I_0, \hbar\omega, \tau_{\rm coh})$ given by [10],

$$\rho_{22} = -\beta_0 \frac{\alpha I_0 \Gamma_x \rho_a d\lambda^5/(32\pi^3 c)}{(\hbar\omega - \mathcal{E}_0)^2 + (\Gamma/2)^2 + \alpha I_0 \Gamma_x \rho_a d\lambda^5/(16\pi^3 c)} \quad (1)$$

where $\beta_0(\hbar\omega)$ is the dimensionless optical absorption parameter describing the spontaneous Co L_3 response, $\alpha = 0.5$ a dimensionless parameter that accounts for the layer-by-layer propagated absorption and stimulation response through the Co film of thickness $d = 25$ nm, I_0 (dimension [energy/(area$\times$time)]) the incident intensity, $\Gamma_x = 0.96$ meV the Co L_3 dipole transition energy width for linearly polarized x-rays, $\rho_a = 90.9$ nm^{-3} the number density of Co atoms, $\lambda = 1.59$ nm the resonant wavelength, $c = 300$ nm/fs the speed of light, and $\Gamma = 430$ meV the core hole energy decay width.

The change of the (in-beam) transmitted intensity due to stimulation relative to the transmitted intensity due to spontaneous processes is given by [8],

$$\frac{I_{\rm t}^{\rm stim}}{I_{\rm t}^{\rm spon}} = \frac{e^{-2[\beta_0(1-2\rho_{22})]kd}}{e^{-2\beta_0 kd}} \quad (2)$$

where $k = 2\pi/\lambda$ is the photon wavevector. The change in first-order diffracted magnetic response is given by [10]

$$\frac{I_{\rm d}^{\rm stim}}{I_{\rm d}^{\rm spon}} = \frac{1 - e^{-2\beta_0(1-2\rho_{22})kd}}{1 - e^{-2\beta_0 kd}}$$
$$\times \frac{\cosh(2\Delta\beta_0[1-2\rho_{22}]kd) - \cos(2\Delta\delta_0[1-2\rho_{22}]kd)}{\cosh(2\Delta\beta_0 kd) - \cos(2\Delta\delta_0 kd)} \quad (3)$$

where $\delta_0(\hbar\omega)$ is the dimensionless spontaneous optical dispersion parameter and $\Delta\beta_0, \Delta\delta_0$ the magnetism induced changes of the optical parameters. The exponential prefactors in (2) and (3) reveal the complementary behavior of in-beam transmitted and out-of beam diffracted intensities which are determined by a change in the spontaneous absorption coefficient β_0 in the presence of stimulation to $\beta_0(1 - 2\rho_{22})$. The last term in

(3) reveals that magnetic diffraction depends on changes in both the absorptive $\Delta\beta_0$ and dispersive $\Delta\delta_0$ magnetic sample response.

The results of our simulations are superimposed on the experimental data in Fig. 3, with single-shot transmission intensities shown as open blue circles and diffraction intensities as open red circles. The origin of the large variance in the stimulated response is mainly due to a combination of the short coherence time and photon energy spread of the individual coherent spikes in the SASE pulses as illustrated in more detail in Fig. 4.
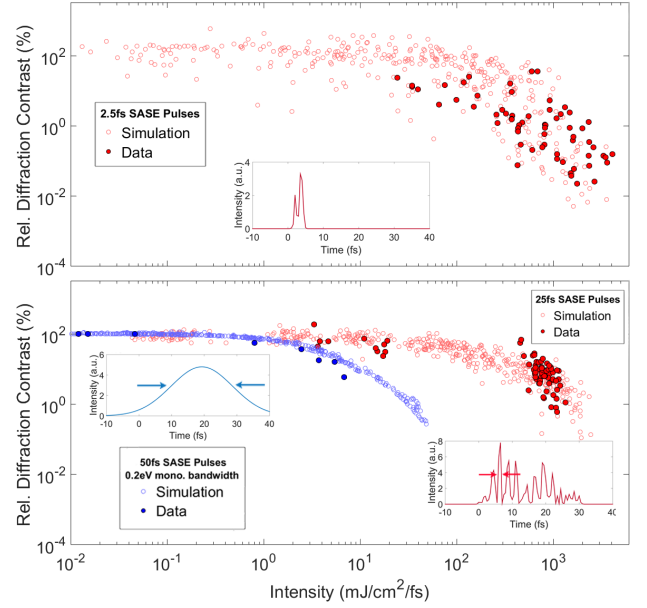

FIG. 4: (color online) Simulations juxtaposed with experimental data for various beam parameters. Top: Simulations and data for 2.5 fs SASE pulses, with a representative simulated pulse plotted in the inset. Bottom: Simulations and data for 25 fs SASE pulses with (blue) and without (red) monochromatization, with representative simulated pulses for both cases plotted in the insets. The response of the longer 25 fs SASE pulses follows the same mean value as the response of the shorter 2.5 fs pulses, but with lower standard deviation by a factor of $\approx \sqrt{10}$, consistent with our independent SASE spike assumption. Monochromatized data utilizing 50 fs pulses are taken from [10].

First, the short intrinsic coherence time of the spikes within the SASE pulses prevents the electronic system from reaching a consistent ρ_{22} value, which is only reached in equilibrium when $\tau_{\rm coh}$ is significantly longer than the femtosecond core hole life time $t_\Gamma = \hbar/\Gamma$ [8]. Second, the different photon energies of the individual spikes lead to a spread in detuning energies $\hbar\omega - \mathcal{E}_0$ in (1) and therefore in ρ_{22}. The energy spread associated with the temporal spikes in a single pulse is enhanced by the shot-by-shot jitter in the central energy of the SASE pulses caused by pulse-to-pulse jitter of the electron beam energy.

By comparison of the experimental and simulated data

shown in red for $\tau_1 = 2.5\,\mathrm{fs}$ and $\tau_2 = 25\,\mathrm{fs}$ pulses in Fig. 4 we see that both pulses have a similar dependence of the diffraction contrast with incident intensity, but the response variance is significantly smaller for the longer pulses. The reduction factor of the variance is found to be close to $\sqrt{\tau_2/\tau_1} = \sqrt{10}$, consistent with the independent SASE spike assumption and the larger number of spikes in the 25 fs pulses that leads to improved noise statistics.

In the bottom half of Fig. 4 we also compare the stimulated response for our non-monochromatic SASE pulses with that of monochromatized pulses recorded by Wu et al. [10], shown in blue. Besides greatly reduced noise due to the longer coherence time of the monochromatic pulses of $\Delta\mathcal{E}_0 = 0.2\,\mathrm{eV}$ (see blue inset), the onset of stimulated diffraction is lowered by a factor of about 100 by the elimination of energy jitter $\hbar\omega - \mathcal{E}_0$ since the photon energy is fixed to the resonance energy by the monochromator. This behavior is in good accord with that predicted by Fig. 2 in Ref. [8].

Our main results are summarized in Fig. 5, where we plot the averaged response signals in both the transmission and diffraction channels, obtained by simple spline fits to the data. The figure reflects the complementary, opposing nonlinear responses in the two channels. The pnCCD diffraction signal is attenuated by 2 orders of magnitude, while forward transmission increases from the spontaneous value of 30% to the stimulated value of $\sim 100\%$.
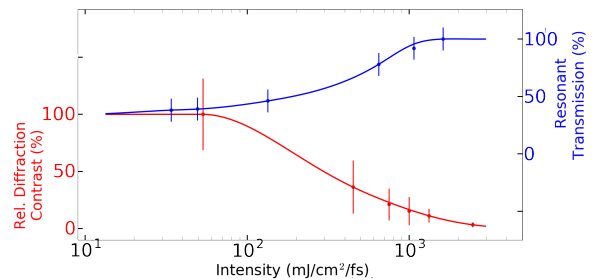

FIG. 5: (color online) Summary results of the observed transmission (blue) and magnetic diffraction (red) contrast relative to the flat conventional spontaneous response as a function of incident intensity.

In summary, our measurements reveal the observation of complete x-ray transparency for a solid sample predicted in Ref. [8]. Together with previous diffraction results [10], our work also reveals the key dependence of stimulated effects on intensity, coherence time, and resonance tuning of the photon energy.

[1] N. Rohringer et al., Nature **481**, 488 (2012).
[2] M. Beye et al., Nature **501**, 191 (2013).
[3] T. Kroll et al., Phys. Rev. Lett. **120**, 133203 (2018).
[4] C. Weninger et al., Phys. Rev. Lett. **111**, 233902 (2013).
[5] J. Stöhr, *NEXAFS Spectroscopy* (Springer, Heidelberg, 1992).
[6] J. Stöhr and H. C. Siegmann, *Magnetism: From Fundamentals to Nanoscale Dynamics* (Springer, Heidelberg, 2006).
[7] J. H. Hubbell, P. N. Trehan, N. Singh, B. Chand, D. Mehta, M. L. Garg, R. R. Garg, S. Singh, and S. Puri, J. Phys. Ref. Data **23**, 339 (1994).
[8] J. Stöhr, A. Scherz: Phys. Rev. Lett. **115**, 107402 (2015); *Phys. Rev. Lett.* **116**, 019902 (2016).
[9] J. Stöhr, Phys. Rev. Lett. **118**, 024801 (2017).
[10] B. Wu, T. Wang, C. E. Graves, D. Zhu, W. F. Schlotter, J. J. Turner, O. Hellwig, Z. Chen, H. A. Dürr, A. Scherz, et al., Phys. Rev. Lett. **117**, 027401 (2016).
[11] O. Hellwig, G. Denbeaux, J. Kortright, and E. E. Fullerton, Physica B: Condensed Matter **336**, 136 (2003).
[12] C. Bostedt, S. Boutet, D. M. Fritz, Z. Huang, H. J. Lee, H. T. Lemke, A. Robert, W. F. Schlotter, J. J. Turner, and G. J. Williams, Rev. Mod. Phys. **88**, 015007 (2016).
[13] J. C. Castagna et al., Journal of Physics: Conference Series **425**, 152021 (2013).
[14] S. Schreck et al., Phys. Rev. Lett. **113**, 153002 (2014).
[15] C. Boeglin et al., Nature **465**, 458 (2010).
[16] V. Shokeen, M. S. Piaia, J.-Y. Bigot, T. Müller, P. Elliott, J. K. Dewhurst, S. Sharma, and E. K. U. Gross, Phys. Rev. Lett. **119**, 107203 (2017).
[17] E. L. Saldin, E. A. Schneidmiller, and M. V. Yurkov, New J. Phys. **12**, 035010 (2010).
[18] R. A. Smith, Proceedings of the Royal Society A: Mathematical, Physical and Engineering Sciences **362**, 1 (1978).
[19] R. A. Smith, Proceedings of the Royal Society A: Mathematical, Physical and Engineering Sciences **362**, 13 (1978).
[20] I. A. Vartanyants et al., Phys. Rev. Lett **107**, 144801 (2011).